Spontaneous Thermal Runaway as an Ultimate Failure Mechanism of Materials

S. Braeck* and Y. Y. Podladchikov

Physics of Geological Processes (PGP), University of Oslo, P.O. Box 1048 Blindern, N-0316 Oslo, Norway

(Received 6 September 2006; published 2 March 2007)

The first theoretical estimate of the shear strength of a perfect crystal was given by Frenkel [Z. Phys. **37**, 572 (1926)]. By assuming that two rigid atomic rows in the crystal would move over each other along a slip plane, he derived the ultimate shear strength to be about one-tenth of the shear modulus. Here we present a theoretical study showing that catastrophic failure of viscoelastic materials may occur below Frenkel's ultimate limit as a result of thermal runaway. The thermal runaway failure mechanism exhibits progressive localization of the strain and temperature profiles in space, thereby producing a narrow region of highly deformed material, i.e., a shear band. We calculate the maximum shear strength σ_c of materials and then demonstrate the relevance of this new concept for material failure known to occur at scales ranging from nanometers to kilometers.

DOI: 10.1103/PhysRevLett.98.095504 PACS numbers: 81.40.Np, 83.60.Bc, 83.60.St, 91.32.−m

It is well known that the shear strength of real crystals is typically several orders of magnitude smaller than Frenkel's ultimate shear strength limit. This discrepancy is explained by the fact that real crystals contain defects such as dislocations which lower the shear strength dramatically. Nevertheless, some materials, like rocks in the Earth's interior and metallic glasses, apparently have strengths approaching Frenkel's theoretical limit. For these materials it is reasoned that the mobility of the defects is in one way or another reduced. For instance, the closure of cracks at high confining pressures, nonplanar crystal structure of minerals and disorder of mineral grain orientations are all factors contributing to the high strength of rocks in the Earth's interior. The high strength of metallic glasses is attributed to the high degree of structural disorder causing dislocations to experience a large number of obstacles, reducing their mobility and inhibiting plastic flow.

However, even if dislocation mobility is greatly reduced, materials subjected to increasing loads do not necessarily fail according to Frenkel's model. When subjected to a high shear stress which approaches, but is reproducibly lower than Frenkel's limit, these materials may fail by deformation localized on a single or a few regions (shear bands) having thicknesses that are orders of magnitude larger than interatomic spacing, but which are still very narrow compared to the deforming sample size. Moreover, this extreme localization of shear is often accompanied by extensive melting and resolidification of the material. This mode of failure is manifested by the so-called pseudotachylytes in geological outcrops (cm thick deformation bands believed to be the traces of large paleoearthquakes) [1,2] and catastrophic failure along ca. 10 nm thick shear bands reported in metallic glasses [3–5].

The occurrence of localized shear zones in the deeper parts of the Earth's lithosphere poses a problem due to its paradoxical nature. Earthquakes are usually attributed to the intrinsic stick-slip character of brittle failure or frictional sliding on a preexisting fault. Brittle failure is expected as the primary mode of rock failure down to 15–20 kms, the so-called seismogenic zone. Because of the high confining pressure at depth, however, these mechanisms alone are not plausible explanations for earthquakes occurring significantly deeper than the seismogenic zone. Several potential rock-weakening mechanisms have instead been proposed to facilitate deep earthquakes, including structural changes such as dehydration embrittlement and olivine spinel phase transition [6] or thermal softening leading to shear instability [7,8]. Recent assessment of these models using indirect seismological evidence argues in favor of a temperature-activated phenomenon, such as thermal shear instabilities, due to apparent temperature dependence of deep earthquakes [9]. Similarly, structural strain softening and thermal softening are possible explanations for shear-band formation in metallic glasses [10,11]. A recent experiment [4], however, revealed that the heated zone associated with an individual band was much wider than the shear band itself. It was concluded [4] that shear-band operation could not be fully adiabatic and temperature rise could not therefore be the factor controlling shear-band thickness, thus rejecting the thermal softening mechanism. In contrast, our work presented below shows that the nonadiabaticity of the thermal softening process may in fact be the cause of strain localization inside the hot zone, and we thus provide an alternative interpretation to the experimental results in Ref. [4].

It is well accepted that even below the conventional elastic limit, most real materials show nonelastic rheological responses such as creep under constant load and stress relaxation under constant extension induced by thermally excited defects and imperfections. In accordance with these properties, most materials may be characterized as viscoelastic; i.e., the rheology contains both viscous and elastic components. Since the phenomena of creep and relaxation are thermally activated processes, the viscosity is strongly temperature dependent (e.g., Arrhenius) and it is, in general, a nonlinear function of the shear stress [12].

The strong temperature dependence of the viscosity has important implications as it leads to thermal softening of the material. Indeed, as first noted by Griggs and Baker [7], such a physical system is inherently unstable: an increase in strain rate in a weaker zone causes a local temperature rise due to viscous dissipation and weakens the zone even further. At high stresses, viscous dissipation becomes substantial, and if heat is generated faster than it is conducted away, the local increase in temperature and strain rate is strongly amplified. Under those conditions a positive feedback between temperature rise and viscous dissipation is established and a thermal runaway develops. To determine whether the thermal runaway mechanism can explain the aforementioned material failure, we approach the problem by considering a simple viscoelastic model which accounts for the nonelastic behavior below the ultimate yield point (Frenkel's limit). The temperature T in the model is determined by the equation for energy conservation which is coupled, through temperature dependent viscosity, to the rheology equation.

Our one-dimensional model (see Fig. 1) consists of a viscoelastic slab of width L at initial temperature T_{bg} except in the small central region having width h and slightly elevated temperature T_0. The boundaries are maintained at the temperature T_{bg}. Our objective is to search for spontaneous modes of internal failure not aided or triggered by the effect of additional far-field deformation. Hence, for time $t \geq 0$ we impose zero velocity v at the boundaries and assume that, without addressing the loading history ($t < 0$), the slab initially ($t = 0$) is subjected to

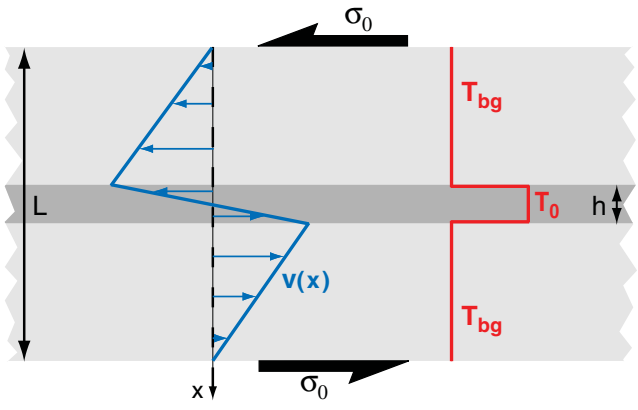

FIG. 1 (color). Initial setup of the viscoelastic slab model discussed in the text (cross section in the xy plane). The slab is in a state of stress of simple shear with zero velocity ($v = 0$) boundary conditions. The shear stress σ, constant throughout the slab, initially ($t = 0$) equals the maximum value σ_0 and subsequently decreases with time due to relaxation and viscous deformation in the interior. The blue and red lines show the initial velocity and temperature profiles, respectively. The shaded region illustrates a small perturbation in temperature T_0 of width h at the slab center. Elsewhere, the background temperature is T_{bg}. The geometry of the strain rate profile concurs with that of the temperature profile.

a shear stress σ_0. The shear stress σ in the slab satisfies the equation for conservation of momentum

$$\frac{\partial \sigma}{\partial x} = 0, \tag{1}$$

which shows that σ is independent of x and hence only a function of the time t. The viscoelastic rheology is represented by the Maxwell model [13], and is given by the equation

$$\frac{\partial v}{\partial x} = \frac{1}{\mu(T, \sigma)}\sigma + \frac{1}{G}\frac{\partial \sigma}{\partial t}, \tag{2}$$

where $v(x, t)$ is the velocity, G is the constant shear modulus, and $\mu(T, \sigma)$ is the viscosity. The dependence of μ on T and σ may be written as

$$\mu(T, \sigma) = A^{-1} e^{E/\mathrm{RT}} \sigma^{1-n}, \tag{3}$$

where A and n are constants, E is the activation energy, and $R = 8.3\ \mathrm{J\,K^{-1}\,mole^{-1}}$ is the universal gas constant. Since $\sigma(t)$ is independent of x, it follows from Eq. (2) that the geometry of the strain rate ($\partial v/\partial x$) profile at any instant concurs with that of the temperature profile $T(x, t)$. Utilizing the zero velocity boundary condition, Eq. (2) may be integrated to obtain the equation which governs the time dependence of σ:

$$\frac{\partial \sigma}{\partial t} = -\frac{\mathrm{GA}}{L}\sigma^n \int_{-L/2}^{L/2} e^{-E/\mathrm{RT}} dx. \tag{4}$$

The temperature is determined by the equation for energy conservation

$$\frac{\partial T}{\partial t} = \kappa \frac{\partial^2 T}{\partial x^2} + \frac{A}{C}\sigma^{n+1} e^{-E/\mathrm{RT}}, \tag{5}$$

where the last term accounts for viscous dissipation in the system. Equations (4) and (5) constitute a closed system of coupled ordinary and partial differential equations for two unknown functions $\sigma(t)$ and $T(x, t)$.

First, to determine the conditions necessary for thermal runaway to occur, a linear stability analysis was carried out. Equation (4) was approximated for the initial stages by substituting the initial conditions for T and σ. This yields a characteristic time $\tau_r = \mu_0/(2G\Delta_p)$ for stress relaxation. Here $\mu_0 \equiv \mu(T_0, \sigma_0)$ and $\Delta_p = h/L + e^{E/\mathrm{RT}_0 - E/\mathrm{RT}_{\mathrm{bg}}}$ is a factor which characterizes the initial perturbation. Linearization of the temperature equation with account of stress relaxation yields that the growth of the perturbation in the initial stages is controlled by the two dimensionless variables τ_r/τ_d and σ_0/σ_c, where the thermal diffusion time $\tau_d = h^2/\kappa$ (κ is the thermal diffusivity) and the newly introduced stress

$$\sigma_c = \sqrt{2\Delta_p \frac{\mathrm{GCR}}{E}} T_0. \tag{6}$$

Here C denotes the heat capacity per volume. The solution

to the linearized temperature equation is found to be unstable if $\sigma_0/\sigma_c > f(\tau_r/\tau_d)$. In the limit $\tau_r/\tau_d \ll 1$, which corresponds to near adiabatic conditions, the function f quickly approaches the lower bound $f \approx 1$ and the solution therefore becomes unstable if $\sigma_0 > \sigma_c$. Thus σ_c is the critical stress above which a thermal runaway may occur and therefore provides an estimate of the maximum shear strength of viscoelastic materials. Initial stages of thermal runaway instability in a more general setup was recently investigated in Ref. [14], including two-dimensional verification of the one-dimensional predictions. The results of our linear stability analysis are in agreement with these numerical estimates in the limit of vanishing boundary velocity.

Nonlinear evolutions of the unstable runaway modes rapidly deviate from the exponential growth in time predicted by linear analysis. Since important information about the deformation process can be inferred from the increase in temperature, we choose the maximum temperature rise $\Delta T_{\max} = T_{\max} - T_0$ during the deformation process as our main physical quantity to study. This enables us to quantify even the later stages of the thermal runaway process not considered in the linear analysis. A simple estimate of $\Delta T_{\max}$ during thermal runaway may be obtained assuming adiabatic conditions. In this case all the elastic energy in the system is uniformly dissipated as heat in the perturbed zone and overall energy balance yields the adiabatic temperature rise

$$\Delta T^a_{\max} = \frac{L\sigma_0^2}{2h\mathrm{GC}}. \tag{7}$$

Guided by these analytical estimates, the complete time evolution of T and σ was subsequently investigated by numerical methods. We simplified the problem by dimensional analysis reducing it from one containing 13 dimensional parameters to one containing six dimensionless parameters. The dimensionless form of the coupled set of Eqs. (4) and (5) were solved numerically using a finite-difference method with nonuniform mesh and a tailored variable time step in order to resolve the highly nonlinear effect of localization. We have systematically varied all six dimensionless parameters and computed $\Delta T_{\max}$ for each temperature evolution. Remarkably, it is possible to present $\Delta T_{\max}$ normalized by the adiabatic temperature rise [Eq. (7)] as a function of only two combinations of parameters, namely σ_0/σ_c and τ_r/τ_d, as previously suggested by the linear stability analysis. A representative set of runs is shown in Fig. 2(a). This "phase diagram" was computed by varying two of the dimensionless parameters and fixing the remaining four. The plot exhibits a low-temperature region corresponding to stable deformation processes, and a high-temperature region corresponding to thermal runaway processes. These regions are sharply distinguished by a critical boundary having a location that correlates well with stability predictions of the linear analysis. The phase diagram is "representative" in that it is insensitive to which two out of the six dimensionless parameters are varied, keeping the remaining four fixed.

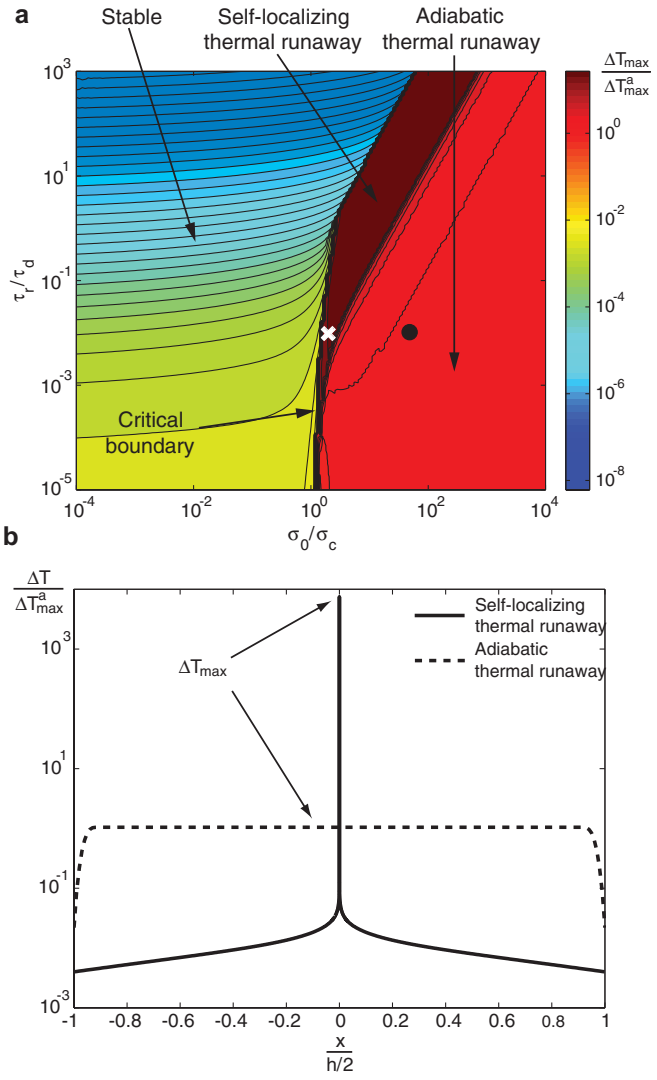

FIG. 2 (color). Dependence of the maximum temperature rise $\Delta T_{\max}$ on the dimensionless variables σ_0/σ_c and τ_r/τ_d. (a) Contour plot of $\Delta T_{\max}$ scaled by the adiabatic temperature rise $\Delta T^a_{\max}$ as a function of σ_0/σ_c and τ_r/τ_d. The dark lines are contour lines. Because of the computational effort of fully resolving the entire self-localizing thermal runaway processes, the temperature at the very late stages of these processes are not presented in this plot. (b) Profiles of the temperature rise $\Delta T = T - T_0$ inside the initially perturbed zone $|x| \leq h/2$ at the time when the maximum temperature is reached. The solid line illustrates the self-localizing thermal runaway process at the location of the cross in (a). The dashed line illustrates the adiabatic thermal runaway at the location of the dot in (a).

In the neighborhood of the critical boundary in the high-temperature region, however, the temperatures are found to be much larger than the adiabatic temperature rise $\Delta T^a_{\max}$. In this region we observe a continuous localization of the temperature and strain profiles during the deformation process; i.e., the runaway is spatially self-localizing. This

localization effect is illustrated for the temperature profile in Fig. 2(b). The elastic energy is thus dissipated in a zone much narrower than the width of the initial perturbation resulting in much larger temperatures. The self-localization of the runaway process arises from the effects of thermal diffusion: by diffusion the temperature profile acquires a peak in the center where the effect of the positive feedback mechanism accordingly is maximized. The runaway therefore accelerates faster in the center than in the regions outside and the deformation process finally terminates in a highly localized shear band with a characteristic width much smaller than the characteristic width h of the initial perturbation.

To evaluate the relevance of thermal runaway as a potential failure mechanism in nature, we now consider two case examples comparing critical stress for thermal runaway with Frenkel's ultimate shear strength limit ($\sigma \sim G/10$). First, we estimate the condition necessary for thermal runaway to occur in olivine-dominated mantle rocks. For olivine (see Ref. [12]) $G = 7 \times 10^{10}$ Pa, $C = 3 \times 10^6$ J m^{-3} K^{-1} and $E = 5,\ 23 \times 10^5$ J mole^{-1}, while we assume $T_{\mathrm{bg}} = 700$ K (corresponding to a depth of about 40 km), $T_0 = 701$–720 K and $h = 10$ m, $L = 10$ km. Substituting these values in Eq. (6) we predict that thermal runaway possibly occurs if the stress exceeds a critical value in the range $\sigma_c = 0.5$–1.7 GPa, i.e., $\sigma_c = G/140 - G/40$. This estimate agrees rather well with the values observed in experimental studies of rock deformation under high confining pressure, where typical failure stresses are in the range 0.5–2 GPa [7,15]. Second, for a metallic glass, typical values are $C = 2,\ 6 \times 10^6$ J m^{-3} K^{-1} (Ref. [4]), $G = 34$ GPa (Ref. [16]), and $E = 100$–400 kJ mole^{-1} (Ref. [17,18]). Assuming $h = 1\ \mu$m, $L = 1$ cm, $T_{\mathrm{bg}} = 300$ K (room temperature), and $T_0 = 301$ K we obtain a critical stress in the range $\sigma_c = 0.4$–1.1 GPa, i.e., $\sigma_c = G/90 - G/30$. For comparison, we note that the shear yield strength of the metallic glass Vitreloy 1 is about 0.8 GPa $= G/40$ [4,16], a value consistent with our estimate of the critical stress necessary for thermal runaway.

The magnitude of the critical stress in these two estimates is remarkably similar considering the very different types of materials discussed and the enormous difference in time and length scales. However, as is evident from Eq. (6), the quantities which govern the kinetic processes in these systems (in particular, the scale h and the poorly constrained viscosity μ) do not appear in the expression for σ_c. It is not surprising, therefore, that the stress required to initiate spontaneous thermal runaway is relatively well constrained to about 1 GPa.

These estimates and the concept of self-localizing thermal runaway demonstrate that our simple model is sufficient to explain failure below Frenkel's ultimate shear strength limit and strain localization at scales much larger than the lattice spacing. The fact that initiation of thermal runaway depends so weakly on the kinetic quantities gives confidence in the application of such models even to the very large scales involved in continental deformation [14,19–21].

The authors thank K. Mair (PGP) and S. Medvedev (PGP) for discussions. This work was supported by the Norwegian Research Council through a Center of Excellence grant to PGP.

*Electronic address: simen.brack@fys.uio.no

[1] T. B. Andersen and H. Austrheim, Earth Planet. Sci. Lett. **242**, 58 (2006).
[2] M. Obata and S. Karato, Tectonophysics **242**, 313 (1995).
[3] W. J. Wright, R. B. Schwarz, and W. D. Nix, Mater. Sci. Eng. A **319–321**, 229 (2001).
[4] J. J. Lewandowski and A. L. Greer, Nat. Mater. **5**, 15 (2006).
[5] C. C. Hays, C. P. Kim, and W. L. Johnson, Phys. Rev. Lett. **84**, 2901 (2000).
[6] H. W. Green and P. C. Burnley, Nature (London) **341**, 733 (1989).
[7] D. T. Griggs and D. W. Baker, *Properties of Matter under Unusual Conditions* (Wiley, New York, 1968).
[8] M. Ogawa, J. Geophys. Res. **92**, 13 801 (1987).
[9] D. A. Wiens, Phys. Earth Planet. Int. **127**, 145 (2001).
[10] A. Molinari and R. J. Clifton, J. Appl. Mech. **54**, 806 (1987).
[11] C. A. Pampillo, J. Mater. Sci. **10**, 1194 (1975).
[12] D. L. Turcotte and G. Schubert, *Geodynamics* (Cambridge University Press, Cambridge, England, 2002), 2nd ed..
[13] L. E. Malvern, *Introduction to the Mechanics of a Continuous Medium* (Prentice-Hall, Englewood Cliffs, NJ, 1969).
[14] B. J. P. Kaus and Y. Y. Podladchikov, J. Geophys. Res. **111**, B04412 (2006).
[15] C. E. Renshaw and E. M. Schulson, J. Geophys. Res. **109**, B09207 (2004).
[16] W. L. Johnson and K. Samwer, Phys. Rev. Lett. **95**, 195501 (2005).
[17] Q. Wang, J. Lu, F. J. Gu, H. Xu, and Y. D. Dong, J. Phys. D **39**, 2851 (2006).
[18] H. S. Chen, Rep. Prog. Phys. **43**, 353 (1980).
[19] K. Regenauer-Lieb, R. F. Weinberg, and G. Rosenbaum, Nature (London) **442**, 67 (2006).
[20] K. Regenauer-Lieb, D. A. Yuen, and J. Branlund, Science **294**, 578 (2001).
[21] M. Kameyama, D. A. Yuen, and S. Karato, Earth Planet. Sci. Lett. **168**, 159 (1999).